PEM FUEL CELL DYNAMIC SIMULATION USING *FuelCell*LIB

M.A. Rubio, A. Urquía, S. Dormido
Dept. Informática y Automática, Universidad Nacional de Educación a Distancia (UNED), Madrid, Spain

Corresponding author: M.A. Rubio, Dept. Informática y Automática, ETS Ingeniería Informática, UNED, Juan del Rosal 16, 28040, Madrid, Spain, marubio@dia.uned.es

Abstract. *FuelCell*Lib is a free Modelica library for 1D dynamic modelling of PEMFC (proton exchange membrane fuel cells). *FuelCell*Lib models describe phenomena that take place in the cell cathode and the membrane, including the electrochemical reactions in the catalytic layer, the electronic conduction in the catalytic and diffusion layers, the protonic conduction in the proton conductor material (e.g., Nafion polymers) of the catalytic layer and the membrane, the coexistence of steam and liquid water, the transport of water in liquid and steam phases, the electro-osmotic drag, the transport of oxygen in steam phase in the catalytic and diffusion layers, the cathode flooding, the membrane drying, and the double-layer capacitance.

The first version of *FuelCell*Lib was released in 2005. The second version of the library, which can be freely downloaded from http://www.euclides.dia.uned.es/, is presented in this manuscript. The modelled phenomena, modelling hypotheses and structure of the library are discussed. In addition, the effect of selected parameters on the voltage response after current interruption: the cell polarization curve, the flow of liquid water in the membrane, the dynamic of the cathode flooding process, and the steady-state spatial distribution of water load and oxygen is analyzed using *FuelCell*Lib.

1 Introduction

Our society is suffering from fossil fuel shortage. Fossil fuels (i.e., coal, oil, and natural gas) also contribute to a number of environmental problems during their extraction, transportation, and use. As an alternative for the devices consuming fossil fuels, fuel cells are one of the most promising means of producing energy in portable systems.

The mathematical modelling of PEMFC (proton exchange membrane fuel cells) is a challenging topic, due to the complexity and variety of phenomena involved in the operation of these devices, including fluid-dynamic of gases and liquids in complex media, electrochemical reactions, heat transfer, and ion conduction in electrolytes. Different approaches to the modelling and simulation of PEMFC are based on the use of different software tools:

1. Computational fluid dynamics (CFD) software, such as FLUENT [1, 2, 3, 4], CFX [5] and STAR-CD [6], has been used for 2D and 3D steady-state modelling of PEMFC.
2. Numerical code written in a programming language such as C, Fortran, etc. For instance, the commercial software GCTool [7] supports the simulation of 0D dynamic models of PEMFC. The LIMEX [8] numerical solver has been used to simulate the 1D dynamic model presented in [9]. The 2D dynamic model proposed in [10] has been simulated by applying the method described in [11] and using a programming language.
3. The Matlab/Simulink simulation environment, which supports block diagram modelling, has been used in [12, 13]. In addition, some commercial tools which use Matlab/Simulink (e.g., Emmeskay [14] and FEMLAB [15]), provide libraries for fuel cell modelling.
4. The capabilities for model reuse [16] provided by object-oriented modelling languages (e.g., Modelica and gPROMS) facilitate the development of libraries of components intended for PEMFC modelling. The Modelica library implemented by Steinmann and Treffinger [17] allows composing 0D steady-state PEMFC models. A 0D dynamic model of PEMFC written in Modelica, suited for real-time simulation, was proposed in [18].

Another Modelica library for PEMFC modelling is *FuelCell*Lib [19, 20]. In contrast with the two aforementioned libraries, *FuelCell*Lib facilitates the 1D dynamic modelling of PEMFC. *FuelCell*Lib models are based on physical-chemical principles. The balances of the species (i.e., water, oxygen, protons and electrons) are enunciated in each physical layer of the fuel cell. The finite volume method has been applied to discretize the PDE in the spatial coordinate perpendicular to the layers. The modelled physical-chemical phenomena include:

– Membrane: transport of water in liquid and steam phase, and protonic conduction.
– Catalytic layer of the cathode: transport of water in liquid and steam phase, transport of oxygen in steam phase, protonic and electronic conduction, and electro-catalytic reaction.
– Diffusion layer of the cathode: transport of water in liquid and steam phase, transport of oxygen in steam phase and electronic conduction.

The first version of *FuelCell*Lib was released in 2005. The second version of the library, which can be freely downloaded from [21], is presented in this manuscript. The modelled phenomena, modelling hypotheses and structure of the library are discussed in Section 2. The effect of selected parameters on the voltage response after current interruption: the cell polarization curve, the flow of liquid water in the membrane, the dynamic of the cathode flooding process, and the steady-state spatial distribution of water load and oxygen is analyzed using *FuelCell*Lib in Section 3.

2 Design of *FuelCell*Lib

The *FuelCell*Lib Modelica library is intended to facilitate the dynamic modelling of PEMFC in the context of automatic control. The modelling hypotheses of *FuelCell*Lib are discussed in Section 2.1. The structure of the library is presented in Section 2.2. The connectors, the atomic components (i.e., models of control volumes and transport phenomena) and the layer models are discussed in Sections 2.3, 2.4 and 2.5, respectively. Cell models are composed by connecting layer models. The interface models used to connect the cell to electric and gas flow components are described in Section 2.6. The obtained 2-layer and 3-layer PEMFC models are described in Section 2.7. These fuel cell models can be connected to the electric load models (Section 2.8) and to models describing boundary conditions on the gas flow (Section 2.9). These experimental setups (Section 2.10) can be used to perform the variety of analyses described in Section 3.

2.1 Modelled phenomena and hypotheses

*FuelCell*Lib models are based on the following considerations and hypotheses:

1. The relevant phenomena take place in the cell cathode [22, 23]. Therefore, the fuel cell model is composed of the membrane, the catalytic layer of the cathode and the diffusion layer of the cathode. *FuelCell*Lib models describe phenomena that take place in the cell cathode and the membrane, including the following:
   - Electrochemical reactions in the catalytic layer.
   - Electronic conduction in the catalytic and diffusion layers.
   - Protonic conduction in the proton conductor material (e.g., Nafion polymers) of the catalytic layer and the membrane.
   - Transport of water in liquid and steam phases.
   - Transport of oxygen in steam phase in the catalytic and diffusion layers.
   - Liquid water flooding in the porous materials.
2. As the models have to represent time-dependent behaviors, they need to be dynamic. Phenomena over a wide time-scale range are considered. For instance, *FuelCell*Lib cell models allow simulating the cell dynamic response to step changes in the load value that occur over time scales of μs, and the voltage drop due to the cathode flooding process that occur over time scales of hours.
3. The fuel cell model is one dimensional. Physical magnitudes change in the direction normal to the surface of the membrane and the electrodes. This allows analyzing the following phenomena: (1) the flow of species to the active areas of the catalytic layer; (2) the conduction of electrons and protons; and (3) the drying and flooding phenomena in the catalytic and diffusion layers, and in the membrane.

   The balances of the species (i.e., water, oxygen, protons and electrons) are enunciated, in each physical layer of the fuel cell, by means of the definition of control volumes. The properties of the medium inside the control volume are considered time-dependent, but independent of the spatial coordinates. The control volumes exchange the different species with their environment through certain control planes. All the interactions between the control volumes are considered transport phenomena in *FuelCell*Lib. The physical layers of the fuel cell (i.e., the membrane and the catalytic and diffusion layers of the cathode) are modelled by decomposition into control volumes, which are connected to each other by means of transport phenomena.
4. The species are indicated in Table 1. The presence of oxygen in the membrane has not been considered. Also, the protonic conduction in the diffusion layer and the electronic conduction in the membrane have not been considered. However, the presence of species in the layers depends on the value given to the transport coefficients of the species. This allows describing the oxygen permeability across the membrane.

Specie	Membrane	Catalytic layer	Diffusion layer
Water in steam phase	X	X	X
Water in liquid phase	X	X	X
Oxygen	-	X	X
Protonic conduction	X	X	-
Electronic conduction	-	X	X

Table 1: Species considered in *FuelCell*Lib.

The diffusion of water in steam and liquid phases, and the diffusion of O_2 in the porous media have been modelled. Also, the phase equilibrium of the water (i.e., steam-liquid equilibrium) in the porous media has been taken into account.

5. *FuelCell*Lib models are isothermal. The temperature dependence of the phenomena is modelled, but the temperature of each layer is uniform and constant during the simulation run. The heat conduction and its generation, due to the electrochemical reactions and the transport of species, are not considered.
6. The hydrogen electrochemical reaction is significatively faster in the anode than in the cathode [22, 23].
7. The hydrogen diffusivity is much higher than the oxygen and air diffusivities. On the other hand, the flooding phenomenon takes place in the cathode. As a consequence, the fuel transport is mainly limited in the cathode.
8. Gases are considered ideal. The movement of gases is due to the concentration gradients and to the gas pressure in the electrodes. The flow speed and the gas pressure gradients are considered small. Therefore, the fluid momentum is conserved.
9. The electrodes, the catalytic layer and the membrane are considered isotropic and homogeneous. Porous media (i.e., catalytic and diffusion layers) are defined by the value of its porosity and tortuosity. The porosity and tortuosity of the porous layers are homogeneous. The catalyzer and the protonic conductor electrolyte are evenly distributed. It is considered only one pore size. These assumptions lead to a macro-homogeneous model [24, 25].
10. The proton concentration inside the proton conductor electrolyte is constant and uniform. As a consequence, the polymeric electrolyte has the properties of an electrical conductor.
11. The library user is allowed to decide whether to include or not the following phenomena in the cell model:
    - Existence of double-layer pseudocapacitance in the catalyst layer.
    - Influence of the pore size in the Knudsen diffusion.
    - Effect of the electro-osmotic drag in the electrolyte.
    - Dependence of the electrolyte conductivity with the water load.

2.2 Library architecture

The structure of the library is shown in Figure 1. It contains the models of the control volumes and transport phenomena (*Atomic Elements* package) used to compose the 1D dynamic models of the cathode and the membrane (*Layer1D* package). Their connection allows composing two-layer (i.e., membrane and catalytic layer) and three-layer (i.e., membrane, catalytic and diffusion layers) models of PEMFC. The interface models (*Interfaces* package) allow connecting the fuel cell models to components describing the gas flow (*Gas_Function* package) and the electric loads (*Loads* package). The gas flow models (*Gas_Function* package) are intended to set the boundary conditions of the gas flow. The *casestudies* package contains some models of experimental setups that can be used to perform a broad variety of simulation experiments.

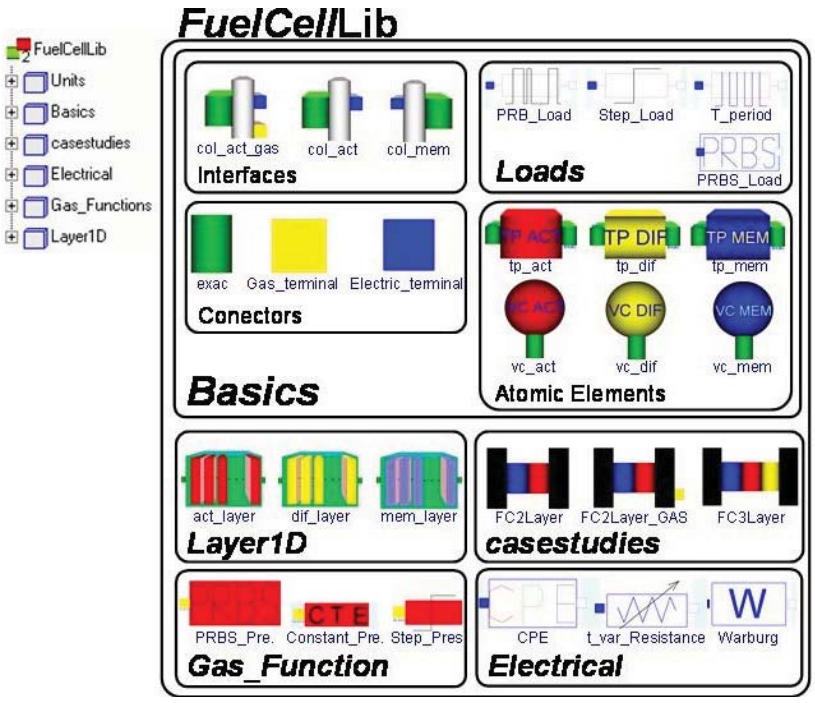

Figure 1: Packages and models of *FuelCell*Lib 2.

2.3 Interaction between components

The interaction between components is modelled by means of the following three types of connectors (see the *Connectors* package in Figure 1):

– The *exac* connector allows to connect the models of the control volumes and the interfaces to the models of the transport phenomena. The definition of this connector is summarized in Table 2. The models contained in the *Atomic Elements* and *Layer1D* packages have this type of connector.

Specie	Across variable	Through variable
Water in steam phase	p_{H_2O}, partial pressure (Pa)	$J^g_{H_2O}$, molar flow (mol·m^{-2}·s^{-1})
Water in liquid phase	$\chi_{s_{H_2O}}$, load (Kg$_{H_2O}$·Kg$^{-1}_{solido}$)	$J^l_{H_2O}$, molar flow (mol·m^{-2}·s^{-1})
Oxygen	p_{O_2}, partial pressure (Pa)	J_{O_2}, molar flow (mol·m^{-2}·s^{-1})
Protonic conduction	V_e, voltage (V)	J_e, current density (A·m^{-1})
Electronic conduction	V_s, voltage (V)	J_s, current density (A·m^{-1})

Table 2: Variables of the *exac* connector.

– The *Electric_terminal* connector allows to connect the electric components. Its variables are shown in Table 3. The models contained in the *Loads* and *Electrical* packages have this type of connector.

Specie	Across variable	Through variable
Electronic conduction	v_s, voltage (V)	J_s, current density (A·m^{-1})

Table 3: Variables of the *Electric_terminal* connector.

– The *Gas_terminal* connector allows to connect the gas flow models to the cell. Its variables are shown in Table 4. The models contained in the *Gas_Functions* package have this type of connector.

Specie	Across variable	Through variable
Oxygen	p_{O_2}, partial pressure (Pa)	J_{O_2}, molar flow (mol·m^{-2}·s^{-1})
Water in steam phase	p_{H_2O}, partial pressure (Pa)	$J^g_{H_2O}$, molar flow (mol·m^{-2}·s^{-1})

Table 4: Variables of the *Gas_terminal* connector.

2.4 Atomic components: control volumes and transport phenomena

The atomic components describing the control volumes and transport phenomena are included within the *Atomic Elements* package (see Figure 1). As it was discussed in Section 2.1, the membrane, the catalytic layer and the diffusion layer are modelled by decomposition into control volumes. The properties of the medium inside the control volume are considered time dependent, but independent of the spatial coordinates.

– The *vc_dif* model describes a control volume of the diffusion layer. It contains the molar balances of oxygen, steam and liquid water. Besides, it contains equations describing that the total electronic flow is zero and the total protonic flow is zero.

– The *vc_act* model describes a control volume of the catalytic layer. It contains the molar balances of oxygen, steam and liquid water. An equation describes the charge balance: the electronic flow generated by the electrochemical reaction is equal to the consumed protonic flow. In addition, a conditional equation allows the user to decide whether to consider or not the existence of a double-layer pseudocapacitance.

– The *vc_mem* model describes a control volume of the membrane. It contains the molar balances of steam and liquid water. As there is neither generation nor consumption of protons, the model contains an equation imposing that the total protonic flow is zero. Also, the electronic voltage of the electrolyte and the oxygen pressure are set to zero.

The three control volume models contain equations for calculating the water saturation pressure.

The flows of species between adjacent control volumes are described by the transport phenomenon models. The properties of a flow that goes out from a control volume depend on the properties of the medium contained inside this control volume. The direction of the flow established between two control volumes depends on the medium properties inside the control volumes.

– The *tp_dif* model describes the flow of oxygen, steam, liquid water and electrons between control volumes of the diffusion layer. As the medium is not a conductor of protons, a very small value has been given to its protonic conductivity. As a result, the protonic conduction is negligible. On the other hand, several alternative expressions describing the Knudsen diffusion are provided. The model user is allowed to choose one of them.

– The *tp_act* model describes the flow of oxygen, steam, liquid water, electrons and protons between control volumes of the catalytic layer. Again, several alternative expressions describing the Knudsen diffusion are provided. Also, several alternative expressions are provided for estimating the protonic conductivity of the electrolyte. The liquid water flow due to the electro-osmotic drag is calculated.
– The *tp_mem* model describes the flow of steam, liquid water and protons between control volumes of the membrane. As it has been assumed that the membrane is impermeable to oxygen and electrons, the flow of these species is set to zero. The flow of liquid water due to the electro-osmotic drag is calculated. Again, several alternative expressions are provided for describing the Knudsen diffusion and estimating the protonic conductivity of the electrolyte.

All atomic components contain equations for calculating the pore size.

2.5 Modelling of the layers

The *Layer1D* package contains the models of the three layers that compose the fuel cell (see Figure 1): the diffusion layer (*dif_layer* model), the catalytic layer (*act_layer* model) and the membrane (*mem_layer* model). Each layer has been composed by alternatively connecting control volume and the transport phenomenon models, as it is shown in Figure 2. The number of control volumes, n, is a model parameter. The length of the inner control volumes is Δx, while the length of the terminal ones is $\frac{\Delta x}{2}$.

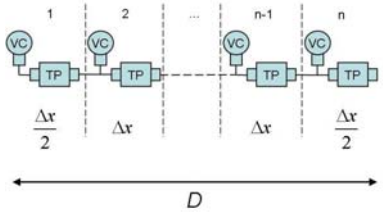

Figure 2: Spatial discretization of a layer.

2.6 Cell interfaces to electric and gas flow components

The models of the *Interfaces* package allow to connect the layer models to other models describing electric components and boundary conditions for the gas flow. The following three types of interface models have been defined (see the *Interfaces* package in Figure 1):

– The *col_mem* model is the electric interface of the anode - i.e., it allows to connect the cell anode to the electric components of *FuelCell*Lib. Also, this interface sets the gas flow boundary conditions on the cell anode, which have to satisfy the following:

1. The oxygen crossover through the membrane is not modelled. Therefore, the partial pressure of oxygen at the cathode has to be zero. On the other hand, the voltage of the solid and the electrolyte are, by convention, equal to zero. These boundary conditions are summarized in Table 5.

Symbol	Description	Value
p_{O_2}	Partial pressure of oxygen	0
J_{O_2}	Oxygen flow	0
v_s	Voltage of the solid	0
v_e	Voltage of the electrolyte	0

Table 5: Boundary conditions derived from the modelling hypotheses.

2. The model user may define boundary conditions on the pressure (p_{H2O}) and flow (J^g_{H2O}) of steam, and on the load ($\chi_{s_{H_2O}}$) and flow ($J^l_{H_2O}$) of liquid water. However, the following restriction must be satisfied: of each pair of terminal variables (i.e. across/through), one have to be calculated from the environment and the other have to be calculated from the cell equations. For instance, if the pressure of steam is a boundary condition for the cell model, then the steam flow have to be calculated from the cell model. Analogously, if the steam flow is a boundary condition, then the partial pressure of steam has to be calculated from the cell model. The same restriction applies to the load and flow of liquid water.

– The *col_act* model is the electric interface of the cathode - i.e., it allows to connect the cell cathode to the electric components of *FuelCell*Lib. Defining a different interface for the anode and the cathode allows setting different values to the anode and cathode overpotentials.

In addition, this interface allows setting boundary conditions on the pressure (p_{O_2}) and flow (J_{O_2}) of oxygen, the pressure (p_{H_2O}) and flow ($J^g_{H_2O}$) of steam, and the load ($\chi_{s_{H_2O}}$) and flow ($J^l_{H_2O}$) of liquid water. The

following restriction must be satisfied: of each pair of terminal variables (i.e. across/through), one has to be calculated from the environment and the other has to be calculated from the cell equations. This interface model contains the equations to calculate the open-circuit voltage of the cell. This voltage is a global variable (i.e., a *outer* variable), which is used by the catalytic layer components.

– The *col_act_gas* model is the interface among the cell cathode, and the electric and gas-flow components. It has the same functionality than *col_act*, allowing also to set boundary conditions on the gas pressures. The components of the *Gas_Function* package (see Figure 1) are used for this purpose. This interface allows setting boundary conditions on the pressure (p_{H_2O}) and flow ($J^g_{H_2O}$) of steam, and the load ($\chi_{s_{H_2O}}$) and flow ($J^l_{H_2O}$) of liquid water. Again, the following restriction must be satisfied: of each pair of terminal variables (i.e. across/through), one has to be calculated from the environment and the other has to be calculated from the cell equations. The oxygen pressure (p_{O_2}) is set by the components modelling the gas flow.

2.7 Fuel cell models

Fuel cell models can be built by connecting the corresponding layer models, and the anode and cathode interface models. An example is shown in Figure 3. The fuel cell model is composed, from left to right, of the anode interface (*col_mem*), the membrane (*mem_layer*), the catalytic layer (*act_layer*), the diffusion layer (*dif_layer*) and the cathode interface (*col_cat*).

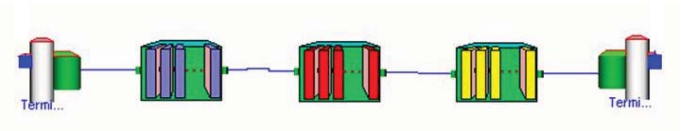

Figure 3: Diagram of a three-layer model of a fuel cell.

2.8 Electric loads

The *Loads* package contains some models of electric loads that are intended to facilitate the modelling of experimental setups. For instance, the *T_period* model represents a periodic, square-wave ohmic resistance, and the *Step_Load* model represents a step change in the ohmic resistance. The *PRB_Load* model represents an ohmic resistance whose value is a pseudorandom binary signal with two levels. The signal holds its value during a time that is is uniformly distributed over a certain interval. The upper limit of this interval can be set by the model user.

2.9 Boundary conditions on the gas flow

The *Gas_Function* package contains models that facilitate setting boundary conditions on the oxygen and steam flows. These models allow to set the gas pressure to a constant value specified by the model user (*Constant_pressure* model), to induce step changes in the gas pressure (*Step_Pressure* model) and to set the pressure value according to a pseudorandom binary signal.

2.10 Modelling experimental setups

The *casestudies* package contains models of experimental setups (see Figure 4), composed by the connection of fuel cell models, electric components and boundary conditions on the gas pressure.

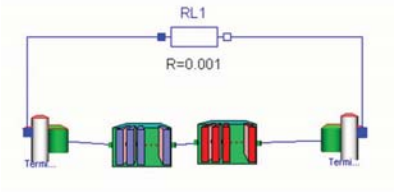

(a) *FC2Layer*.

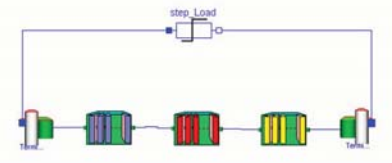

(b) *FC3Layer*.

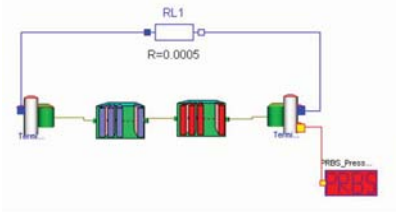

(c) *FC2Layer_gas*.

Figure 4: Models of the *casestudies* package.

The diagram of the *FC2Layer* model is shown in Figure 4a. The fuel cell model is composed of two layers - the membrane (*mem_layer*) and the catalytic layer (*act_layer*) -, and the anode (*col_men*) and cathode (*col_cat*) interfaces. The electric load is the resistance model of the Modelica standard library.

The *FC3Layer* model, whose diagram is shown in Figure 4b, is composed of a three-layer model of a fuel cell and an electric component that generates a step change in the load.

A third experimental setup is included in the *casestudies* package: the *FC2Layer_gas* model (see Figure 4c). In this case study, the model *col_cat_gas* is used as cathode interface and the model *Pressure_PRBS* is used to set the oxygen pressure. The electric load is the resistance model of the Modelica standard library.

2.11 Simulation of the cell polarization curve

Two Modelica script files are provided inside the *casestudies* directory: *pol_curve_FC2.mos* and *pol_curve_FC3.mos*. They automatically calculate the polarization curve of the two-layer and three-layer models of the fuel cell, respectively. To do so, these script files automatically launch the required simulation runs, using in each case a different value of the electric load. Each simulation run is executed until the steady-state is reached. The steady-state value of the cell current and voltage define the point of the polarization curve that corresponds to the load value.

3 Qualitative analysis of the PEMFC behavior using *FuelCell*Lib

*FuelCell*Lib models are used to perform several qualitative analyses of the PEMFC behavior. The effect of selected parameters on the voltage response after current interruption (Section 3.1), on the cell polarization curve (Section 3.2) and on the dynamic of the cathode flooding process (Section 3.4) is investigated. Also, the effect of considering the electro-osmotic drag is analyzed (Section 3.3). Finally, the effect of the current density on the steady-state distribution of water and oxygen is studied (Section 3.5).

3.1 Response to a step change in the electric load

The experimental setup shown in Figure 5 allows studying the cell response to a step change in the electric load. The load and the cell are described by the *Step_Load* and *FC2Layer* models, respectively. The cell response depends on the value of the double-layer capacitance (C_{dl}).

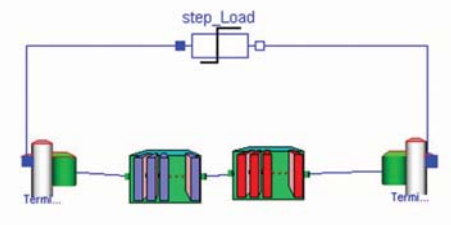

Figure 5: Experimental setup to study the cell response to a step change in load.

The initial value of the load resistance is $10^{-2}\Omega$. The load resistance changes to $10^{6}\Omega$ at time 0.5 s, producing the current interruption. The experiment has been repeated for four different values of the double-layer capacitance: 0, 0.5, 1 y 2 C. The obtained cell voltage is shown in Figure 6.

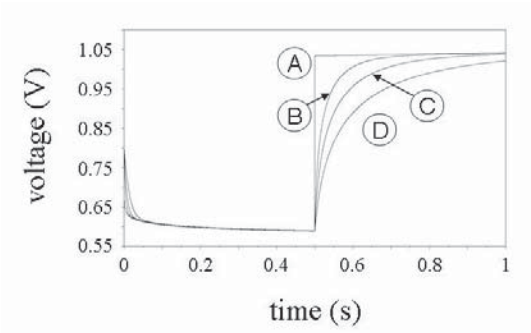

Figure 6: Cell voltage in response to a step change in the load. C_{dl}= 0 C (A), 0.5 C (B), 1 C (C), 2 C (D).

The double-layer capacitance represents the capacity of the interface between the electrolyte and the electronic conductor. The greater the pseudocapacitance, the slower the cell dynamic. The obtained results agree with the results obtained by other authors [29, 12].

3.2 Polarization curve

The effect on the polarization curve of selected design and operating parameters has been analyzed. In particular, the effect of the Tafel slope, the exchange current and the oxygen pressure at the cathode are discussed below.

The I-V curves corresponding to different values of the Tafel slope (b_T) are shown in Figure 7. The Tafel slope influences the rate of the electrochemical reaction. The smaller the Tafel slope, the smaller the activation overpotential. The simulated results are in agreement with the theoretical results [30, 22].

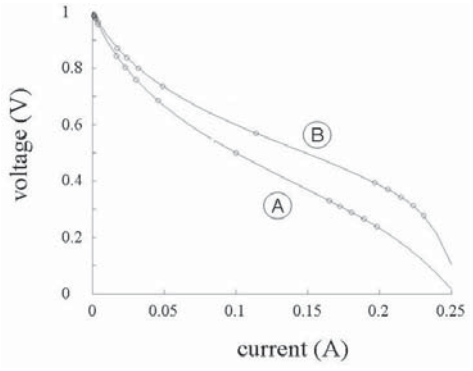

Figure 7: Effect of the Tafel slope (b_T) on the polarization curve. b_T= 0.2 mV (A), 0.15 mV (B).

The exchange current represents the catalytic reaction activity. It mainly depends on the type of catalyzer employed [30]. The estimation of the exchange current can be made using three different hypotheses, which influence the cell polarization curve (see Figure 8). The polarization curve (A) is obtained by neglecting the effect of the oxygen partial pressure on the limit current. The limit current is a constant (J_l). The exchange current (i_o) is calculated from the following expression: $i_o = i_o^{ref}\,(1 - J_e/J_{lim})$. The polarization curve (B) is obtained by assuming that the limit current depends on the oxygen partial pressure. In this case, the exchange current (i_o) is calculated from the following expression: $i_o = i_o^{ref}\left(1 - \frac{J_e}{\left(p_{O_2}/p_{O_2}^0\right)J_{\lim}}\right)$. The polarization curve (C) is obtained from considering that the exchange current is constant, $i_o = i_o^{ref}$.

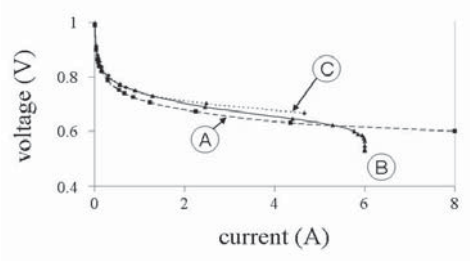

Figure 8: Polarization curves obtained assuming that: (A) the limit current is constant; (B) the limit current depends on the oxygen partial pressure; and (C) the exchange current does not depend on the limit current.

Finally, the polarization curves obtained from considering three different partial pressures of oxygen at the cathode are shown in Figure 9. The greater the partial pressure of oxygen, the smaller the influence of the mass defect phenomenon at high current densities. The obtained results are in agreement with the experimental data [23, 31].

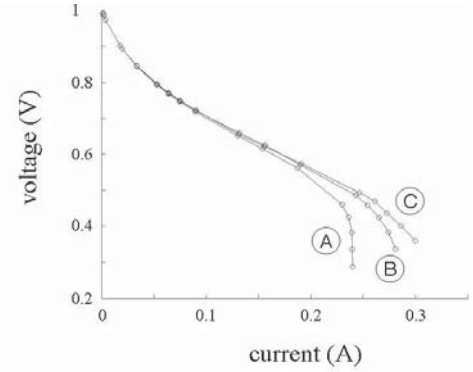

Figure 9: Polarization curves. Partial pressure of oxygen at the cathode: p_{O_2}= 1 atm (A), 2 atm (B), 3 atm (C).

3.3 Electro-osmotic drag

The three-layer model of the cell (*FC3Layer*) is used to analyze the effect of the electro-osmotic drag in the electrolyte. In order to obtain a high current density, it is used a small load resistance: $10^{-5}\Omega$. The water load in the boundaries is set to zero during the simulation run. The steady-state load of water along the spatial dimension is shown in Figure 10 and the flow of liquid water in the center of the membrane in Figure 11. The obtained results indicate that the electro-osmotic drag increases the flow of liquid water from the membrane to the diffusion layer.

The negative sign of the flow indicates that it is directed toward the membrane boundary condition. The flow component due to the electro-osmotic drag has positive sign. The electro-osmotic drag contribution to the flow reduces the absolute value of the total flow. The simulation results indicate that high current densities (and consequently high protonic currents) may produce the membrane drying.

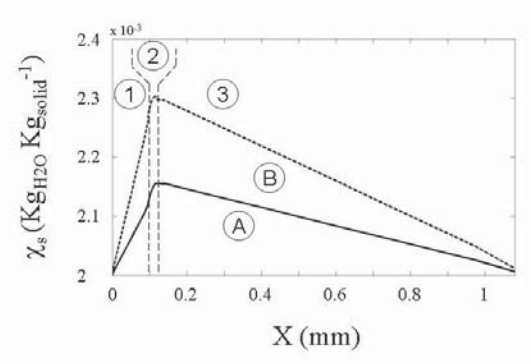

Figure 10: Water load along the spatial dimension: membrane, 10^{-4}m (1), catalytic layer, $2.5 \cdot 10^{-5}$m (2) and diffusion layer 10^{-3}m (3). Without (A) / With (B) electro-osmotic drag.

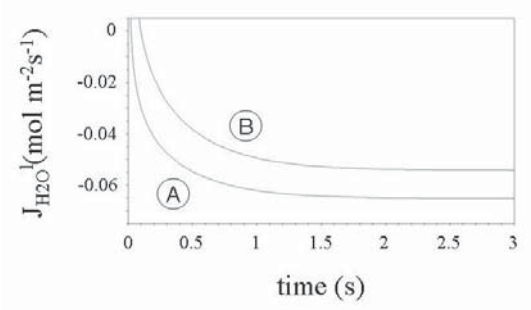

Figure 11: Flow of liquid water in the center of the membrane. Without (A) / With (B) electro-osmotic drag.

3.4 Cathode flooding

The effect of selected parameters on the cathode flooding is investigated. These parameters are the following: the initial load of water accumulated inside the cell (χ_s), the diffusion coefficient of the oxygen in the catalytic layer (D_{O_2K}), the catalytic area and reference exchange current density (Ai_{oref}), the membrane thickness (d_a^{mem}), the catalytic layer thickness (d_a^{act}) and the tortuosity of the catalytic layer (τ).

The two-layer cell model has been used to perform the simulations. The flow of steam and liquid water is set to zero at the cell boundaries. As a consequence, the liquid water generated by the electrochemical reaction remains inside the cell. The cell voltage increases in the early stage of the water accumulation process. This increment is a result of the membrane hydratation and the consequent increment in the membrane conductivity. However, as the water starts flooding the porous material of the active layer, the opposite effect is observed (i.e., the cell voltage decreases).

The hydratation process is significatively faster (one or two orders of magnitude faster) than the flooding process in real fuel cells. However, as the purpose of this simulation study is to analyze qualitatively these two phenomena, the simulated experimental conditions have been selected so that both processes take approximately the same time. The parameter values of the fuel cell model used to analyze the flooding process are shown in Table 6. The simulation results are shown in Figure 12. A detailed discussion on the results can be found in [20].

3.5 Current density

The *FC3Layer* model is used to analyze the steady-state spatial distribution of liquid water that correspond to different values of the current density. The cell layers have the same thickness than in Figure 10. Four different values of the electric load have been used: 10^{-3} Ω, 10^{-4} Ω, 10^{-5} Ω y $5 \cdot 10^{-6}\Omega$. The water load at the boundaries is set to 0.002 $Kg_{H_2O}Kg_{solid}^{-1}$. This value is also used as the initial water load along the cell. Each experimental

Description	Symbol	Value	Units
Membrane thickness	d_a^{mem}	100	μm
Catalytic layer thickness	d_a^{act}	0.8	μm
Catalytic area, reference exchange current density	Ai_{oref}	0.5	A m^{-3}
Knudsen diffusion coef. of oxygen in the catalytic layer	D_{O_2K}	$0.07853 \cdot 10^{-6}$	m^{2}s^{-1}
Water load	χ_s	0.03	$\mathrm{Kg}_{H_2O}\mathrm{Kg}_{solid}^{-1}$
Tortuosity	τ	5	-

Table 6: Parameters of the fuel cell model used to analyze the flooding process.

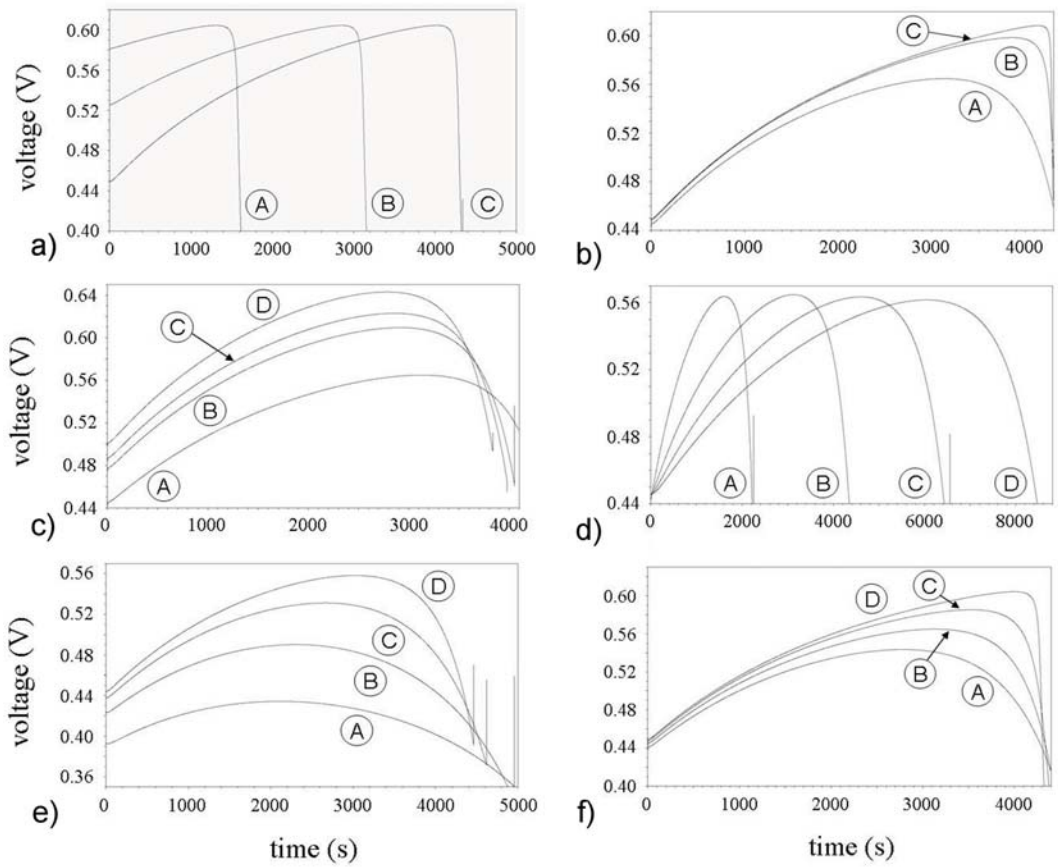

Figure 12: Effect of cell parameters on the flooding process. Nominal value of parameters shown in Table 6. (a) χ_s = 0.08 (A), 0.05 (B), 0.03 (C) $\mathrm{Kg}_{H_2O}\mathrm{Kg}_{solid}^{-1}$; (b) $D_{O_2K} = 2.8{\cdot}10^{-9}$ (A), $2.8{\cdot}10^{-8}$ (B), $2.8{\cdot}10^{-7}$ (C) m^{2}s^{-1}; (c) Ai_{oref} = 0.5 (A), 0.85 (B), 1 (C), 1.28 (D) A m^{-3}; (d) $d_a^{mem} = 0.5 \cdot 10^{-4}$ (A), 10^{-4} (B), $1.5{\cdot}10^{-4}$ (C), $2{\cdot}10^{-4}$ (D) m; (e) $d_a^{act} = 8 \cdot 10^{-6}$ (A), $4{\cdot}10^{-6}$ (B), $2{\cdot}10^{-6}$ (C), $1{\cdot}10^{-6}$ (D) m; and (f) τ = 7 (A), 5 (B), 3 (C), 1 (D).

setup is simulated until the steady-state is reached. The steady-state spatial distribution of liquid water is shown in Figure 13. The higher the current density, the faster the flooding process. As the current density and the generated amount of water are proportional, this was the expected result.

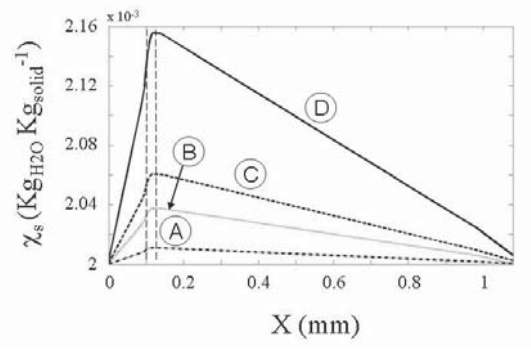

Figure 13: Steady-state spatial distribution of liquid water. J_e= 0.119 A·cm^{-2} (A), 0.404 A·cm^{-2} (B), 0.650 A·cm^{-2}(C), 1.643 A·cm^{-2} (D).

Finally, the two-layer model of the fuel cell is used to obtain the steady-state concentration of oxygen in the catalytic layer. The oxygen pressure at the catalytic layer boundary is set to 10^4 Pa during all the simulation run. The results obtained from four different values of the current density are shown in Figure 14. The higher the current density, the smaller the partial pressure of oxygen in the catalytic layer. This result agrees with the simulation results obtained by other authors [23].

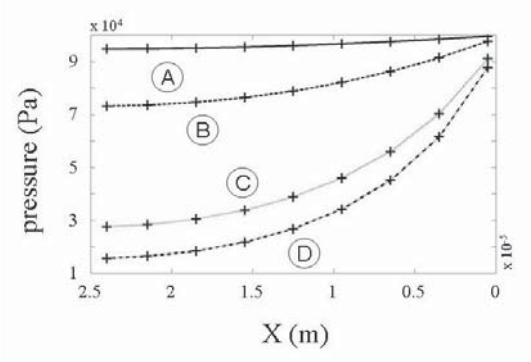

Figure 14: Steady-state partial pressure of O_2 along the catalytic layer corresponding to different current densities: 0.069 A·cm^{-2} (A), 0.413 A·cm^{-2} (B), 1.744 A·cm^{-2} (C), 2.487 A·cm^{-2} (D).

4 Conclusions

*FuelCell*Lib is a free Modelica library intended for 1D dynamic modelling of PEMFC (proton exchange membrane fuel cells). The first version of the library was released in 2005. The second version was presented in this manuscript and it is freely available at http://www.euclides.dia.uned.es/.

*FuelCell*Lib models allow reproducing relevant PEMFC phenomena, including the cathode flooding, the membrane drying, the electro-osmotic drag, the diffusion of liquid and gases through porous media, the coexistence of steam and liquid water, the electrochemical reactions in the cathode, and the double layer capacitance.

The effect of physical and electrochemical parameters on relevant cell phenomena has been discussed in this manuscript. To this end, the PEMFC models and test benches have been composed using *FuelCell*Lib. As a conclusion, *FuelCell*Lib allows enhancing the understanding of the physical-chemical phenomena involved in the PEMFC operation and therefore it is a useful tool for optimizing the PEMFC performance.

5 Acknowledgment

This work has been supported by the Spanish CICYT under DPI2007-61068 grant.

6 References

[1] Hontan E., Escudero M.J., Bautista C., Garca-Ybarra P.L. and Daza L.: *Dynamic model of solid polymer fuel cell water management*. J. Power Sources, 86 (2000), 363-368.

[2] Dutta S. and Shimpalee S.: *Three-dimensional numerical simulation of straight channel PEM fuel cells*. J. Appl. Electrochem. Soc.,30 (2) (2000)

[3] Pasaogullari U. and Wang C.Y.: *Computational fluid dynamics modeling of proton exchange membrane fuel cell using Fluent*. In: Proc. Fluent User Group Meeting, Manchester, 2002.

[4] Kumar A. and Reddy R.G.: *Stainless steel as a bipolar plate material for solid polymer fuel cells*. J. Power Sources, 113 (2002), 11–18.

[5] Berning T., Lu D.and Djilali N.: *Three-dimensional computational analysis of transport phenomena in a PEM fuel cell*. J. Power Sources, 106 (2002), 284–294.

[6] Wang Y. and Wang C.Y.: *Dynamics of polymer electrolyte fuel cells undergoing load changes*. Electrochemica Acta, 51 (2006), 3924–3933.

[7] GCTool *General Computational Toolkit for Fuel Cell Analysis*. Open Channel Foundation, (2007), http://www.openchannelfoundation.org/

[8] Nowak U.: *LIMEX*. Zuse Institute Berlin, (1999), http://www.zib.de/nowak/limex4.html

[9] Whör M., Bolwin K., Schnurnberger W., Fischer M., Neubrand W. and Eigenberger G.: *Dynamic modelling and simulation of a polymer membrane fuel cell including mass transport limitation*. Int. J. of Hydrogen Energy, 23,3 (1998), 213–218.

[10] Natarajan D. and Van Nguyen T.: *A two-dimensional, two-phase, multicomponent, transient model for the cathode of a proton exchange membrane fuel cell using conventional gas distributors*. J. Electrochem. Soc., 148 (12) (2001), 1324–1335.

[11] Nguyen T.V. and White R.E.: *A finite difference procedure for solving coupled, nonlinear elliptic partial differential equations*. J. Electrochem. Soc., 148 (12) (2001), 1324–1335.
[12] Ceraolo M., Miulli C. and Pozio A.: *Modelling static and dynamic behaviour of proton exchange membrane fuel cells on the basis of electro-chemical description*. J. Power Sources, 113 (2003), 131–144.
[13] Golbert J. and Lewin D.R.: *Model-based control of fuel cells: (1) Regulatory control*. J. Power Sources, 135 (2008), 135–151.
[14] Emmeskay: *Fuel Cell stack users manual*. Emmeskay INC., (2008), http://www.emmeskay.com/products/fuel-cell-stack model/
[15] FEMLAB: *Chemical Engineering Module*. FEMLAB, Comsol, (2008), http://www.comsol.com/products/chem/
[16] Astrom K.J., Elmqvist H. and Mattsson S.E.: *Evolution of continuous-time modeling and simulation*. In: Proc. 12^{th} European Simulation Multiconference, 1998, Manchester, UK.
[17] Steinmann W.D. and Treffinger P.: *Simulation of Fuel Cell Powered Drive Trains*. In: Proc. Modelica Workshop, 2000, Lund, Sweden.
[18] Ungethüm J.: *Fuel Cell System Modeling for Real-time Simulation*. In: Proc. 4^{th} Int. Modelica Conference, 2005, Hamburg, Germany.
[19] Rubio M.A., Urquia A., Gonzalez L., Guinea D. and Dormido S.: *FuelCellLib - A Modelica Library for Modeling of Fuel Cells*. In: Proc. 4^{th} Int. Modelica Conference, 2005, Hamburg, Germany.
[20] Rubio M.A.: *Modelado Dinámico de Pilas de Combustible en el Contexto del Control Automático*. PhD Dissertation, Dept. Informática y Automática, UNED, Madrid, Spain, 2008.
[21] Dept. Informática y Automática, UNED, Madrid, Spain, *Some Free Modelling & Simulation Resources:* http://www.euclides.dia.uned.es/
[22] Bevers D., Wöhr M. and Yasuda K.: *Simulation of polymer electrolyte fuel cell electrode*. J. Appl. Electrochem. Soc., 27(11) (1997), 1254–1264.
[23] Broka K. and Ekdunge P.: *Modelling the PEM fuel cell cathode*. J. Appl. Electrochem. Soc., 27(3) (1997), 281–289.
[24] Bernardi D.M. and Verbrugge M.W.: *A Mathematical Model of the Solid-Polymer-Electrolyte Fuel Cell*. J. Electrochem. Soc., 139(9) (1992), 2477-2491.
[25] Springer T.E. and Zawodzinsky T.A.: *Polymer Electrolyte Fuel Cell Model*. J. Electrochem. Soc., 138(8) (1991), 2334–2342.
[26] Urquia A. and Dormido S.: *Object-oriented design of reusable model libraries of hybrid dynamic systems - Part two: A case study*. Mathematical and Computer Modelling of Dynamical Systems, 9(1) (2002), 91–118.
[27] Bird R.B., Stewart W.E. and Lightfoot E.N.: *Transport Phenomena*. John Wiley & Sons, New York, 1975.
[28] Incropera F.P. and DeWitt D.P.: *Fundamentals of Heat and Mass Transfer*. John Wiley & Sons, New York, 1996.
[29] Peng J., Shin J.Y. and Song T.W.: *Transient response of high temperature PEM fuel cell*. J. Power Sources, 179 (2008), 220–231.
[30] Larminie J. and Dicks A.: *Fuel cell systems explained*. John Wiley & Sons, New York, 2000.
[31] Yan Q., Toghiani H. and Causey H.: *Steady state and dynamic performance of proton exchange membrane fuel cells (PEMFCs) under various operating conditions and load changes*. J. Power Sources, 161 (2006), 492–502.
[32] Brenan K.E., Campbell S.L. and Petzold L.R.: *Numerical Solution of Initial-Value Problems, Differential-Algebraic Equations*. SIAM, 1996.